

Identifying overlapping terrorist cells from the Noordin Top actor-event network

Saverio Ranciati^{*,*}, Veronica Vinciotti[†] and Ernst C. Wit[‡]

Saverio Ranciati
Department of Statistical Sciences
University of Bologna
Via delle Belle Arti 41, Bologna, 40127
Italy
e-mail: saverio.ranciati2@unibo.it

Veronica Vinciotti
Department of Mathematics
Brunel University London
Uxbridge UB8 3PH
The UK
e-mail: veronica.vinciotti@brunel.ac.uk

Ernst C. Wit
J.B.I. for Mathematics and Computer Science
University of Groningen
Nijenborgh 99747 AG Groningen
The Netherlands
e-mail: e.c.wit@rug.nl

Abstract: Actor-event data are common in sociological settings, whereby one registers the pattern of attendance of a group of social actors to a number of events. We focus on 79 members of the Noordin Top terrorist network, who were monitored attending 45 events. The attendance or non-attendance of the terrorist to events defines the social fabric, such as group coherence and social communities. The aim of the analysis of such data is to learn about this social structure. Actor-event data is often transformed to actor-actor data in order to be further analysed by network models, such as stochastic block models. This transformation and such analyses lead to a natural loss of information, particularly when one is interested in identifying, possibly overlapping, subgroups or communities of actors on the basis of their attendances to events. In this paper we propose an actor-event model for overlapping communities of terrorists, which simplifies interpretation of the network. We propose a mixture model with overlapping clusters for the analysis of the binary actor-event network data, called **manet**, and develop a Bayesian procedure for inference. After a simulation study, we show how this analysis of the terrorist network has clear interpretative advantages over the more traditional approaches of network analysis.

Keywords and phrases: Bayesian modeling, mixture models, MCMC algorithm, network, overlapping clusters.

^{*}corresponding author.

1. Introduction

Networks are an intuitive and a powerful way to describe interactions among individuals in many fields of application. In social sciences, for example, network structures describe concisely the observed relationships among people, tribes, social media accounts and so forth. A recent review about statistical methods and models used in this research area can be found in [Kolaczyk \(2009\)](#). Most of the literature on modelling network data can be grouped into three main branches, with some natural overlapping between the categories: stochastic block models, exponential random graph models, latent space models. Stochastic block models (SBMs) date back to the work of [Holland, Laskey and Leinhardt \(1983\)](#), where the idea of modeling partitions of the network, called blocks or *communities*, was first introduced. Since then, numerous extensions, such as mixed memberships and dynamic networks, have been proposed ([Wang and Wong, 1987](#); [Nowicki and Snijders, 2001](#); [Airoldi et al., 2008](#); [Xing et al., 2010](#)). Another way to summarize a network structure is to model the amount of sub-structures, in a graphical and topological sense, comprising the network itself. This approach has been formulated as the exponential random graph model in the early work of [Frank and Strauss \(1986\)](#); see also [Wasserman and Pattison \(1996\)](#) and [Robins et al. \(2007\)](#) for a review of some recent developments. Finally, the last framework deals with individuals in the network and their relations by projecting them into a latent space, where the probability of interaction between units is modeled based on their distance in this non-observable representation ([Hoff, Raftery and Handcock, 2002](#)). Recent extensions of this model allow incorporating more complex features of the data, such as dynamic evolution ([Handcock, Raftery and Tantrum, 2007](#); [Raftery et al., 2012](#); [Durante and Dunson, 2014](#); [Sewell et al., 2017](#)).

The approaches mentioned above can be used on network data where all nodes, or actors, are of the same nature. Some network data, however, are provided in the form of attendances of individuals, *actors*, to *events*. These data are also called two-mode networks, bipartite graphs, or affiliation networks ([Wasserman and Faust, 1994](#), Chapter 8). Examples of these networks include: people visiting movies, nations belonging to alliances and co-sponsorships of legislative bills; see [Doreian, Batagelj and Ferligoj \(2004\)](#) for references. A well-known two-mode network collected by [Davis et al. \(1941\)](#) concerns a group of 18 women in the Southern US attending socio-political events, which has been subject of a meta-analysis by [Freeman \(2002\)](#) comparing 21 different methods.

In the literature, there are only a few models that deal directly with this actor-event organization of the network, such as [Aitkin, Vu and Francis \(2017\)](#), who proposed a Rasch model approach. In most cases transformation procedures are used to change *actor-event* data to *actor-actor* data. A recent example is [Signorelli and Wit \(2017\)](#), who provide a penalized approach for network data representing co-sponsorships of legislative bills in the Italian Parliament. Transforming the data has the inherent drawbacks of information loss ([Neal, 2014](#)). In addition, in many situations, it is of prime interest to identify clusters, *communities*, of individuals within the network according to their preferences to attend

specific events instead of being based on how they interact with each other. Parallel to SBMs for *actor-actor* data, there is then the need of a clustering model for *actor-event* data, whereby an actor (unit) is allocated into a community (cluster) based on the probability of attendance to the various events. Differently to SMBs, however, we expect these communities to potentially overlap with each other. Thus, this paper proposes a mixture model formulation that accommodates this assumption and that can be applied directly to actor-event data.

2. Motivating example: Noordin Top terrorist network

In this paper we consider the Noordin Top terrorist network dataset, which contains information about 79 terrorists and their activities in Indonesia and nearby areas, covering the period from 2001-2010 (Everton, 2012; Aitkin, Vu and Francis, 2017). The network revolved around Noordin Mohammad Top, also known as ‘Moneymen’, his main collaborator Azahari Husin, and their affiliates. Data were periodically collected by the International Crisis Group (2009) in an exhaustive qualitative format. Information was later summarized by Everton (2012) into relationships between terrorists, attendances to events and individual data on each terrorist, such as level of education, nationality, etc. The two-mode *actor-event* network model focuses on the recorded attendances of the 79 terrorists to the 45 events. These could be meetings of the Noordin Top network, actual bombings and attacks, or trainings and other operational situations. In particular, we have: eight organizational meeting (*ORG*), five operations, i.e. bombings (*OPER*), eleven training events (*TRAIN*), two financial meetings (*FIN*), seven logistics meetings (*LOGST*) and twelve events generically categorized as ‘meetings’ (*MEET*).

One salient feature of the network is its sparsity, as can be seen in Figure 1a. Figure 1b shows how there are some terrorists and events capitalizing most of the connections. It is believed that a network of terrorists often operates by communities within the networks itself, whereby the individual terrorists are organized according to their role and contribution to the different activities of the whole group. More importantly, it is likely individuals do not belong to a single community, but to more sub-structures in the network. The aim of this paper is to develop a model which can identify how terrorists organize to form such structures.

3. Model formulation

The driving idea is to use a model-based clustering approach to identify clusters of terrorists (*actors*) within the network, based on their attendances to events of different nature (bombings, trainings, financial meetings and so forth), by allowing for these communities to be potentially overlapped. We name the proposed model *multiple allocation model for network data* (**manet**).

3.1. Traditional model-based clustering with finite mixture model

Data are organized in an $n \times d$ matrix of observations y_{ij} , pertaining to n individuals and their attendances to d events. Each element y_{ij} is a binary random variable, with $y_{ij} = 1$ if subject i attends event j . We assume there exist K sub-populations of individuals with cluster proportions $\alpha = (\alpha_1, \dots, \alpha_K)$. In the traditional setting, where clusters are mutually exclusive, this vector satisfies the conditions (i) $\alpha_k \geq 0$, for each k , and (ii) $\sum_{k=1}^K \alpha_k = 1$ (Aitkin, Vu and Francis, 2017). The task is to group together units sharing the same preferential attendance to the d events. Given the binary nature of response variables y_{ij} and assuming independence, the marginal density of an observed attendance profile can be represented by $\mathbf{y}_i | (\alpha, \pi, K) \sim \sum_{k=1}^K \alpha_k \prod_{j=1}^d \text{Ber}(y_{ij}; \pi_{kj})$, with $\mathbf{y}_i = (y_{i1}, y_{i2}, \dots, y_{ij}, \dots, y_{id})$ the attendance profile of the i -th individual to the d events and cluster specific parameters for the probability of attendance, π_{kj} , collected in π . A hierarchical representation is available after introducing a unit-specific latent variable $\mathbf{z}_i = (z_{i1}, \dots, z_{iK})$: if unit i belongs to cluster k , the vector is full of zeros except for the k -th element $z_{ik} = 1$, so $P(z_{ik} = 1) = \alpha_k$ and $\sum_{k=1}^K z_{ik} = 1$, leading to the equivalent hierarchical conditional representation

$$\mathbf{z}_i | \alpha \sim \text{Multinom}(\alpha_1, \dots, \alpha_K), \quad \mathbf{y}_i | (\mathbf{z}_i, \pi_k) \sim \prod_{j=1}^d P(y_{ij} | z_{ik} = 1, \pi_{k:z_{ik}=1}).$$

For each individual i , the model assumes the attendances to events j and j' to be independent from one another, for all $j, j' = 1, \dots, d$ and $j \neq j'$.

3.2. Multiple allocation model for network data (manet)

In many cases, one is interested in groups that are not mutually exclusive, allowing an actor to be allocated simultaneously to potentially more than a single cluster of the mixture model. This problem has been addressed in the statistical literature by mixture models with overlapping clusters (Ranciati, Viroli and Wit, 2017). In order to cluster *actor-event* data by allowing possible overlaps, we relax conditions (ii) on the proportions α and the condition regarding the allocation vector, $\sum_{k=1}^K z_{ik} = 1$ for each i . Each individual will be allowed to belong to any number of the K classes. The number of all possible group membership configurations is equal to $K^* = 2^K$. Instead of working with the latent variables \mathbf{z}_i , we define a new K^* -dimensional allocation vector \mathbf{z}_i^* that satisfies $\sum_{h=1}^{K^*} z_{ih}^* = 1$. We can establish a 1-to-1 correspondence between \mathbf{z}_i and \mathbf{z}_i^* . In general, we introduce a $K^* \times K$ binary matrix U , with $z_{ih}^* = \mathbb{1}_{[\mathbf{u}_h = \mathbf{z}_i]}$, with \mathbf{u}_h denoting the h -th row of U .

For example, when $K = 2$ individual i may be assigned to the first cluster, $\mathbf{z}_i = (1, 0)$, the second cluster $\mathbf{z}_i = (0, 1)$, both of them $\mathbf{z}_i = (1, 1)$ or none

$\mathbf{z}_i = (0, 0)$ and we have

$$U = \begin{pmatrix} 0 & 0 \\ 1 & 0 \\ 0 & 1 \\ 1 & 1 \end{pmatrix}.$$

We can now switch from a mixture model with K overlapping *parent* clusters to a finite mixture of K^* non-overlapping *heir* clusters. Given our new assumptions on the proportions of the *parent* mixture model, the model formulation changes to

$$\mathbf{y}_i | (\boldsymbol{\alpha}^*, \boldsymbol{\pi}^*, K) \sim \sum_{h=1}^{K^*} \alpha_h^* \prod_{j=1}^d \text{Ber}(y_{ij}; \pi_{hj}^*),$$

where now $P(z_h^* = 1) = \alpha_h^*$ and $\boldsymbol{\pi}_h^*$ are the attendance probabilities for the d events for units whose distribution function is given by the non-overlapping cluster h . We specify a conjugate Dirichlet distribution for the proportions $\boldsymbol{\alpha}^*$, that is $P(\boldsymbol{\alpha}^* | \mathbf{a}) = \text{Dir}(a_1, \dots, a_{K^*})$. From $\boldsymbol{\alpha}^*$ we can always compute back the overlapping proportions $\boldsymbol{\alpha}$ with $\alpha_k = \sum_{h=1}^{K^*} \alpha_h^* u_{hk}$.

In order for the overlapping mixture model to have any use and purpose, the original *parent* cluster parameters should affect the *heir* cluster parameters. In particular, the probability π_{hj}^* for *heir* cluster h of attending event j should depend on the parameters $\{\pi_{kj} \mid u_{hk} = 1\}$ of the *parent* clusters involved in the formation of *heir* cluster h . This can be done in a number of ways, which is described more in detail in the next paragraph.

Linking parent and heir cluster parameters

We define the probability to attend event j when belonging to heir cluster h through a function $\psi(\boldsymbol{\pi}_j, \mathbf{u}_h) : \mathbb{R}^K \times \{0, 1\}^K \rightarrow \mathbb{R}$, so that we can compute π_{hj}^* by looking at which parent clusters originated h , through the vector \mathbf{u}_h , and combining their corresponding probabilities $(\pi_{1j}, \dots, \pi_{Kj})$. By changing the definition of ψ one can give different interpretations of the probabilities of attending events when belonging to a multiple allocation cluster.

In this paper we consider the minimum function, whereby we set the probability of attendance for the empty cluster to zero,

$$\pi_{hj}^* = \psi(\boldsymbol{\pi}_j, \mathbf{u}_h) = \begin{cases} \min \{\pi_{kj} \mid u_{hk} = 1\} & \text{if } \sum_k u_{hk} > 0 \\ 0 & \text{if } \sum_k u_{hk} = 0 \end{cases}.$$

For the simple case that $K = 2$, an individual i belonging to both clusters, $\mathbf{z}_i = (1, 1)$, deciding whether to attend an event j or not, will do so by following the lowest ‘preference’ for that specific event, that is $\psi(\pi_{1j}, \pi_{2j}) = \min(\pi_{1j}, \pi_{2j})$. From a Venn diagram perspective, we are implying multiple allocation heir clusters to be intersections of the parent clusters originating them, intersections that are however ‘smaller’ than the parent clusters themselves. In addition, under this combining function $\psi = \min\{\cdot\}$, individuals attending few events will tend to be allocated into multiple allocation heir clusters.

It is worth noting that other choices are possible. For example, setting $\psi = \max\{\cdot\}$ will tend to allocate units with a high number of attendances into multiple allocation clusters. In this case, the set intersections defined by ψ will usually be ‘bigger’ than the parent clusters originating them. Finally, while we pay the price of increasing the number of proportions from K to K^* , these new quantities π^* are not additional parameters and they can be computed from the *parent* parameters π without increasing the parameter space’s dimensionality.

3.3. Bayesian inference

The updated hierarchical formulation of non-overlapping mixture is given by

$$\begin{aligned} P(\alpha^*|\mathbf{a}) &= \text{Dir}(a_1, \dots, a_{K^*}), & P(\pi|\mathbf{b}_1, \mathbf{b}_2) &= \prod_{k=1}^K \prod_{j=1}^d \text{Beta}(\pi_{kj}; b_{1kj}, b_{2kj}) \\ P(\mathbf{z}_i^*|\alpha^*) &= \prod_{h=1}^{K^*} (\alpha_h^*)^{z_{ih}^*}, & P(\mathbf{y}_i|\mathbf{z}_i^*, \pi) &= \prod_{h=1}^{K^*} \prod_{j=1}^d \left[\text{Ber}(y_{ij}; \pi_{hj}^*) \right]^{z_{ih}^*}. \end{aligned}$$

Following this structure, the joint complete data likelihood of the non-overlapping clusters model is

$$\begin{aligned} \mathcal{L}(\alpha^*, \pi; \mathbf{y}, \mathbf{z}^*) &= \prod_{i=1}^n \left\{ \prod_{h=1}^{K^*} \left[\alpha_h^* \prod_{j=1}^d \text{Ber}(y_{ij}; \pi_{hj}^*) \right]^{z_{ih}^*} \right\} \\ &= \prod_{h=1}^{K^*} \left(\alpha_h^* \right)^{n_h^*} \prod_{h=1}^{K^*} \prod_{i: z_i^*=h} \prod_{j=1}^d \text{Ber}(y_{ij}; \pi_{hj}^*) \\ &= \mathcal{L}_{\mathbf{z}^*}(\alpha^*) \mathcal{L}_{\mathbf{y}, \mathbf{z}^*}(\pi), \end{aligned}$$

where $n_h^* = \sum_{i=1}^n z_{ih}^*$ and the product $\prod_{i: z_i^*=h}$ involves only units allocated to cluster h . The second term, $\mathcal{L}_{\mathbf{y}, \mathbf{z}^*}(\pi)$, is a function of the parameters π through the computed quantities π^* . In order to devise a Gibbs sampler for π , we consider the equivalent representation for the overlapping-clusters mixture, as a function of the original *parent* parameters, that is $\mathcal{L}(\alpha^*, \pi; \mathbf{y}, \mathbf{z})$. The first term is equivalent in both parametrization thanks to the 1-to-1 correspondence between \mathbf{z} and \mathbf{z}^* , and the computability of α from α^* . We focus now on the second term of the factorization, $\mathcal{L}_{\mathbf{y}, \mathbf{z}}(\pi)$, as it is not immediately straightforward to define an equivalence. We introduce a new quantity $\mathbf{s}(\mathbf{z}_i, \pi) = \mathbf{s}_i^{(j)}$, whereby $\mathbf{s}_i^{(j)} = \mathbf{z}_i$ if $\sum_{k=1}^K z_{ik} = 1$. Whereas, if $\sum_{k=1}^K z_{ik} > 1$ and if we use the minimum operator, i.e. $\psi = \min(\cdot)$, then $\mathbf{s}_i^{(j)}$ is a K -dimensional vector of zeros except for $s_{ik_{\min, j}} = 1$, with $k_{\min, j}$ denoting the cluster with the lowest value among all the parameters π_k for a fixed event j . In other words: if a unit i belongs to only one cluster (let’s say, k) it will fully contribute to the posterior of the corresponding π_{kj} ; but, if the unit i is allocated into more than one group its contribution will be given only to the lowest parameter $\pi_{k_{\min, j}}$ among all the

relevant attendance probabilities $\{\pi_{kj} \mid u_{h(i)k} = 1\}$ for that j -th event. This definition is compatible with the minimum operator ψ . For other operators, one needs to consider other solutions.

This leads to a convenient factorization of the complete data likelihood of the mixture in the K space:

$$\mathcal{L}(\boldsymbol{\pi}, \mathbf{s}; \mathbf{y}, \mathbf{z}) = \prod_{k=1}^K \prod_{j=1}^d \pi_{kj}^{\sum_{i=1}^n y_{ij} s_{ik}^{(j)}} (1 - \pi_{kj})^{\sum_{i=1}^n s_{ik}^{(j)} - \sum_{i=1}^n y_{ij} s_{ik}^{(j)}}.$$

A sketch of our sampling scheme is the following. For each unit i and *heir* cluster h , we compute the posterior probabilities of allocation according to

$$P(\mathbf{z}_i^* = h \mid \mathbf{y}, \boldsymbol{\alpha}^*, \boldsymbol{\pi}) = \frac{\alpha_h^* \prod_{j=1}^d \text{Ber}(y_{ij}; \pi_{hj}^*)}{\sum_{h'=1}^{K^*} \alpha_{h'}^* \prod_{j=1}^d \text{Ber}(y_{ij}; \pi_{h'j}^*)},$$

and we sample new latent allocation values for \mathbf{z}_i^* . The proportions $\boldsymbol{\alpha}^*$ are updated through the corresponding full conditional distribution, $\boldsymbol{\alpha}^* \sim \text{Dir}(n_1^* + a_1, \dots, n_{K^*}^* + a_{K^*})$. Thanks to the prior-likelihood conjugacy, each of the π_{kj} are updated via a Gibbs sampler with

$$\pi_{kj} \sim \text{Beta}\left(\sum_{i=1}^n y_{ij} s_{ik}^{(j)} + b_{1kj}; \sum_{i=1}^n s_{ik}^{(j)} - \sum_{i=1}^n y_{ij} s_{ik}^{(j)} + b_{2kj}\right).$$

We implement all the samplers in an MCMC algorithm. The latter is also part of the R package `manet`, available on CRAN.

3.4. Selecting the number of clusters and criterion to allocate units

We select the Deviance Information Criterion (Spiegelhalter et al., 2002, DIC) as the model selection criterion. In the DIC, two quantities are balanced, namely the goodness-of-fit and the complexity of the model. In this paper, we rely on the version DIC₃ proposed in Celeux et al. (2006), as the original version does not deal properly with latent variables:

$$\text{DIC}(K) = -4\text{E}_{\boldsymbol{\alpha}^*, \boldsymbol{\pi}}[\log P(\mathbf{y} \mid \boldsymbol{\alpha}^*, \boldsymbol{\pi})] + 2 \log \hat{P}(\mathbf{y}),$$

where both terms can be computed starting from the values sampled at each iteration $t = 1, \dots, T$ of the MCMC algorithm. In particular,

$$\text{E}_{\boldsymbol{\alpha}^*, \boldsymbol{\pi}}[\log P(\mathbf{y} \mid \boldsymbol{\alpha}^*, \boldsymbol{\pi})] = \frac{1}{T} \sum_{t=1}^T \sum_{i=1}^n \log \left\{ \sum_{h=1}^{K^*} \alpha_h^{*(t)} \prod_{j=1}^d \text{Ber}(y_{ij}; \pi_{hj}^{*(t)}) \right\},$$

and

$$\hat{P}(\mathbf{y}) = \prod_{i=1}^n \hat{P}(\mathbf{y}_i), \text{ where } \hat{P}(\mathbf{y}_i) = \frac{1}{T} \sum_{t=1}^T \left\{ \sum_{h=1}^{K^*} \alpha_h^{*(t)} \prod_{j=1}^d \text{Ber}(y_{ij}; \pi_{hj}^{*(t)}) \right\}.$$

In a set of competing models, differing from one another only by K , we select the one with the lowest associated $\text{DIC}(K)$ value.

After the choice of K and, implicitly, K^* , units are allocated into clusters according to their average posterior probabilities and the maximum-a-posteriori (MAP) rule: that is, individual i will be assigned to cluster h showing the highest value for $\bar{P}(z_i^* = h | \mathbf{y}, \boldsymbol{\alpha}, \boldsymbol{\pi}) = T^{-1} \sum_{t=1}^T P(z_i^* = h | \mathbf{y}, \boldsymbol{\alpha}^{(t)} \boldsymbol{\pi}^{(t)})$, computed after initial burn-in window. This post-processing of the posterior helps the interpretation of the results.

3.5. Quantifying clustering uncertainty

As a measure of uncertainty about the clustering provided by the algorithm, we define a quantity called posterior confusion matrix (PCM), whose entry PCM_{hk} stands for the average number of actor with maximum posterior allocation h that will be allocated to k . The PCM is a non-symmetrical $K^* \times K^*$ matrix computed as follows. For each MCMC iteration $t = 1, \dots, T$ and summed across all units $i = 1, \dots, n$, we do the following steps:

1. Order the posterior probabilities $P(z_i^* = h | \mathbf{y}, \boldsymbol{\alpha}^{(t)} \boldsymbol{\pi}^{(t)})$ from highest to lowest, and collect them in a vector $\boldsymbol{\tau}_i^{(t)}$;
2. Define $\mathbf{r}_i^{(t)}$ as the vector of cluster labels associated to $\boldsymbol{\tau}_i^{(t)}$, so that $r_{i,1}^{(t)}$ is the label of the cluster with highest posterior probability (which is $\tau_{i,1}^{(t)}$) for unit i at iteration t among all the K^* possible ones;
3. Add posterior probability $\tau_{i,1}^{(t)}$ to the PCM at position $(r_{i,1}^{(t)}, r_{i,1}^{(t)})$, so that the diagonal element of the matrix account for the first choice of allocation of unit i at iteration t ;
4. While keeping row $r_{i,1}^{(t)}$ fixed as a pivotal quantity of this step, add the remaining probabilities $\tau_{i,2}^{(t)}, \tau_{i,3}^{(t)}, \dots, \tau_{i,K^*}^{(t)}$ to the corresponding positions in the PCM matrix $(r_{i,1}^{(t)}, r_{i,2}^{(t)}), (r_{i,1}^{(t)}, r_{i,3}^{(t)}), \dots, (r_{i,1}^{(t)}, r_{i,K^*}^{(t)})$.

To average the cumulative sums at each position of the matrix, we divide the PCM by the total number of MCMC iterations T . The non-rescaled version of the matrix has row sums equal to the number of units in each corresponding cluster. When rescaled by these row sums, the benchmark matrix for comparison is the identity matrix of order K^* , corresponding to a situation with no uncertainty in the classification.

4. Simulation study

In our simulation study we compare the following algorithms: (i) the proposed model, **manet**, which uses a finite mixture of Bernoulli distributions with overlapping components (as implemented in the package **manet**); (ii) a finite mixture model of Bernoulli distribution with $K = K^*$ non-overlapping components, named **mixtbern**, (iii) a variational method implementing the MixNet model of

Daudin, Picard and Robin (2008), implemented in the R package `mixer`, which is a special case of the binary SBM proposed by Nowicki and Snijders (2001) and (iv) `blockmodels`, proposed by Leger (2015).

4.1. Data generating process

We generate data according to our model with varying values for the number of actors n , the number of events d and the number of clusters K . We consider $K = 3$ (i.e. $K^* = 8$) and set the components weights to be $\alpha^* = (0.1, 0.25, 0.20, 0.1, 0.15, 0.1, 0.05, 0.05)$. We set the probabilities of attendances for the first event equal to $\pi_{\cdot 1} = (0.2, 0.5, 0.9)$ and we define the remaining vectors to be all the possible $(K! - 1)$ permutations of the values in $\pi_{\cdot 1}$, by stacking the same values a number of times depending on the value of d chosen.

Since `blockmodels` and `mixer` only work on *actor-actor* data, for these two methods we transform the data to this structure by calculating the number of events attended by any two actors. This is sufficient for `blockmodels`, which accounts for weighted edges. Since `mixer` requires a binary input, we further dichotomize the network by setting a cutoff on the number of events. We select the threshold that leads to the best results for each of the methods.

4.2. Classification performance

First we evaluate the performance of the methods in terms of classification ability of the actors in the 8 *heir* clusters. For this simulation, we set $n = 300$ and consider three possible values for the number of events, namely $d = \{6, 18, 38\}$. For each of the three values of d , we generate 25 independent datasets. For this simulation, we present the true number of clusters to the algorithms, i.e. $K = 3$ for our model or $K^* = 8$ for the competitors. To measure the performance of the four models we apply the MAP rule to the estimated probabilities of allocation and we cluster units accordingly. After the classification is performed, we compute the average misclassification error rate and the adjusted Rand index (Rand, 1971) for each of the four models across the 25 replicates. The misclassification error rate measures the fraction of units wrongly allocated with respect to the true allocations used to generate the data, whereas the adjusted Rand index (ARI) is a measure between 0 and 1 representing similarity between two different clustering, where we take one of the two to be the true allocation pattern in the data.

Table 1 reports the results of this simulation. In each sub-group defined by the value of d , our model achieves simultaneously lower (better) average misclassification error rate and higher (better) average adjusted Rand index with respect to the other competitors. The closest in terms of performance is `mixtbern`, which however exhibits less stability. It is worth noticing that as the number of events, d , increases so does the performance improvement in the classification task: this is true for all the models except `mixer`. The loss of performance for models `blockmodels` and `mixer` is partially expected due to the loss of information after transformation of the data into a one-mode network.

Misclassification error rate (in %)				
Num. of events	actor-actor		actor-event	
	blockmodels	mixer	mixtbern	manet
$d = 6$	55.49 (3.11)	52.16 (2.23)	42.67 (5.96)	35.05 (3.99)
$d = 18$	43.07 (4.49)	46.89 (5.87)	20.89 (2.97)	15.33 (2.42)
$d = 36$	30.28 (4.76)	54.32 (7.32)	13.67 (4.14)	6.91 (1.53)

Adjusted Rand index ($\text{ARI}_{\max} = 1$)				
Num. of events	actor-actor		actor-event	
	blockmodels	mixer	mixtbern	manet
$d = 6$	0.22 (0.04)	0.15 (0.03)	0.34 (0.08)	0.45 (0.06)
$d = 18$	0.40 (0.06)	0.31 (0.08)	0.73 (0.05)	0.79 (0.04)
$d = 36$	0.60 (0.06)	0.27 (0.08)	0.85 (0.05)	0.93 (0.02)

TABLE 1

Average misclassification error rate (as a percentage) and average adjusted Rand index, summarized over 25 replicated datasets, for three values of $d = \{6, 18, 36\}$ and four competing models; standard errors are reported between brackets. Models are categorized on the type of structure they analyze (actor-actor or actor-event); best results highlighted in bold.

4.3. Convergence of parameters' posterior distributions

In this section we focus on the convergence behavior of the posterior distributions of the attendance probabilities π_{kj} to the true values that produced the data. In particular, we use a fixed setting with $K = 3$, $d = 18$, letting the sample size vary as $n = \{100, 250, 500\}$. We set the true values for the $\{\pi_{kj}\}$ as described in Section 4.1. For each sample size, we simulate 25 replicated datasets and we collect all posterior samples (after burn-in) of the same n from each MCMC into one single chain. While this inevitably introduces some additional Monte Carlo error, the increased amount of available information should dampen this aggregation effect. Results are visualized in Figure 2. Rows of the plot grid correspond to events (specifically, we are reporting $j = \{1, 9, 18\}$) and columns are the attendance probabilities of those event for the three different primary clusters. As expected, increasing sample size (from $n = 100$, red curve, to $n = 500$, blue curve) the posterior distribution exhibits less variability, contracting around the true value, i.e., the vertical dashed line, used for the simulations. The same behavior is observed for the posterior distributions of the other π_{kj} and the posterior distribution of α^* , the proportions of the mixture model (not shown).

4.4. Accuracy of model selection criterion

To show the behaviour of the DIC selection criterion discussed in Section 3.4, we simulate 25 replicated datasets with the following configuration: $K_{\text{true}} = 3$, $d = 18$, increasing sample sizes $n = \{25, 75, 150, 300\}$. For each dataset, we run the algorithm and provide three different values of $K = \{2, 3, 4\}$. We compute the corresponding DIC values and select K achieving the lowest one. When $n = 25$, we select $\hat{K} = K_{\text{true}} = 3$ in 80% of the replicated datasets; for the rest

of the sample sizes $n = \{75, 150, 300\}$, the DIC achieves its lowest value with $\hat{K} = K_{\text{true}} = 3$ in all the datasets.

5. Noordin Top terrorist network analysis

We analyze the terrorist dataset with information pertaining to $n = 79$ terrorists (*actors*) and their attendance behavior to $d = 45$ events of various nature, such as trainings, operations, bombings, financial and logistics meetings, together with their affiliations to a number of organizations, associated with the leader of the Indonesian terrorist network Noordin Top (Everton, 2012). Rather than leaving out the five lone wolf terrorists, we include them into the analysis.

We run our `manet` algorithm for 30,000 iterations with a generous burn-in window of 15,000, to ensure convergence and in order to compute posterior quantities on samples not affected by label-switching. The lowest computed DIC value for three possible values of $K = \{2, 3, 4\}$ corresponds to $\text{DIC}(2) = 6637.3$, and we therefore select $K = 2$ *parent* clusters, corresponding to $K^* = 4$ *heir* clusters.

The results are reported in Table 2. The first *heir* cluster, identifying units belonging to no *parent* cluster, contains 5 units who are the ‘lone wolves’ attending no event and discarded in Aitkin, Vu and Francis (2017) from their analysis. Only two units are allocated into the second *heir* cluster: these two individuals are Noordin Top and Azhari Husin, the leader and his main collaborator of the terrorists network, respectively. They form a separate cluster because of their peculiar behavior of participating to most of the 45 events, having the highest raw number of attendances, respectively 23 and 17, and being involved in many of the logistic, financial, and decision-making meetings. The third *heir* cluster is formed by 6 individuals sharing the same pattern of attendances and, in particular, being terrorists affiliated to a specific sub-group called ‘KOMPAK’. Finally, in the fourth *heir* cluster we find the rest of the terrorists such as trainees, henchmen, and religious leaders, who attend the 45 events with a pattern that is an overlap between the two *parent* clusters.

For comparison, we explore results from our direct competitor `mixtbern`. In both models with $K = 4$ and $K = 8$, only three clusters are non-empty and the partitioning of the units into these mutually exclusive groups is as follows: 77 units into cluster 1, one unit (Noordin Top) into cluster 2, and one unit (Azhari Husin) into cluster 3. This suggests that the potential overlapping of the terrorists groups and patterns in attending events allowed by `manet` helps in identifying better the subgroups in the network. In addition, we can find similarities and differences with the analysis in Aitkin, Vu and Francis (2017). Firstly, in both analyses, aside from the ‘lone wolves’, data seem to point towards a 3-groups structure. Secondly, while the ‘lone wolves’ are removed in the analysis of Aitkin, Vu and Francis (2017), we are able to naturally account for terrorists belonging to the network but showing no attendances to the events considered. Finally, Azhari Husin and Noordin Top are allocated together into a two-units group in both analyses, but terrorists’ memberships to the other two

Clusters		N. of individuals
<i>parent</i> cluster	<i>heir</i> cluster	
$z = (0, 0)$	$h = 1$	5
$z = (0, 1)$	$h = 2$	2
$z = (1, 0)$	$h = 3$	6
$z = (1, 1)$	$h = 4$	66
		79

TABLE 2

Posterior allocation of the 79 terrorists into $K^ = 4$ heir clusters according to maximum-a-posterior (MAP) rule. First column shows the corresponding latent representation in the original parametrization.*

remaining clusters are more confused in Aitkin, Vu and Francis (2017) than with our model in terms of posterior allocations (see Figure 10 of their manuscript).

5.1. Visualizing results and performances

Figure 4 visualizes the two-mode (*actor-event*) Noordin Top network: red square vertexes are the events, with corresponding labeling; round vertexes are the terrorists, with a color scheme representation based on the clustering obtained with **manet**, and labelled with progressive numbers. Figure 3 provides a graphical representation of the posterior probabilities averaged across the MCMC iterations (after burn-in). Each dot represents one of the 79 terrorists (the ‘lone wolves’ are removed for visualization purposes): lower – from left to right – axis of the ternary plot depicts the posterior probability to be allocated into a multiple allocation cluster $z_i = (1, 1)$; similarly, the other two axes (left and right) measure the posterior probability to be allocated into cluster $z_i = (0, 1)$ – top to bottom – or cluster $z_i = (1, 0)$ – bottom to top. We can see almost all units bear no uncertainty about their membership to the clusters, except for two terrorists, row 25 and 55 of the matrix. In order to report the uncertainty of the classification for all the groups, we provide the (PCM) in Table 3. As we see from the table, the results are close to a situation with no confusion in the classification except for cluster $z_i = (0, 0)$. This is partially expected because the data matrix is very sparse and units in the multiple allocation cluster $z_i = (1, 1)$ attend very few events. This means that the attendance profile, and the cluster-specific vector of event probabilities π_h , for cluster $h = 1$ and $h = 4$ are indeed very similar, pushing the algorithm to distinguish less the two groups. However, as we saw in Table 2, the ‘lone wolves’ are classified into cluster $z_i = (0, 0)$, without any additional unit attending a low number of events.

6. Conclusions

In this paper, we have presented a novel finite mixture model and have shown its applicability to the clustering of actor-event data. We formulate the model in such a way that the actor-event data can be modeled directly without transforming it to the more traditional actor-actor network data, with the inherent

Rescaled PCM with $K = 2$ ($K^* = 4$)				
Cluster	$z = (0, 0)$	$z = (0, 1)$	$z = (1, 0)$	$z = (1, 1)$
$z = (0, 0)$	0.66	0.00	0.00	0.34
$z = (0, 1)$	0.00	1.00	0.00	0.00
$z = (1, 0)$	0.00	0.00	0.94	0.06
$z = (1, 1)$	0.01	0.00	0.01	0.98

TABLE 3

Rescaled posterior confusion matrix of the classification for 79 terrorists; the benchmark for comparison (best case scenario) is the identity matrix of order 4.

loss of information. The general formulation with potentially overlapping clusters allows for actors to belong to multiple communities. In particular, we have found out that the Noordin Top terrorist network, besides 5 lone wolf suicide bombers, consisted of a large group of 74 terrorists with within two distinct subgroups: the first consisting of 6 members of the KOMPAK terrorist organization and the second consisting of the 2 leaders, namely Top and Husin. This view of the terrorist network gives a more layered understanding of the mode of operation and allegiances within the organization.

We selected a Bayesian inference procedure for calculating the posterior distribution of the parameters in the model. By selecting appropriate conjugate prior distributions the MCMC sampler is efficient and convergence is typically fast. The proposed model is currently implemented in the R package `manet`, available on CRAN. This Bayesian formulation easily allows extending the model with individual level covariates for group membership or event attendance probabilities.

Acknowledgements

The authors would like to acknowledge the contribution of the COST Action CA15109, called COSTNET, which funded a visit of the first author to Brunel University London.

References

- AIROLDI, E. M., BLEI, D. M., FIENBERG, S. E. and XING, E. P. (2008). Mixed membership stochastic blockmodels. *Journal of Machine Learning Research* **9** 1981–2014.
- AITKIN, M., VU, D. and FRANCIS, B. (2017). Statistical modelling of a terrorist network. *Journal of the Royal Statistical Society: Series A (Statistics in Society)* **180** 751–768.
- CELEUX, G., FORBES, F., ROBERT, C. P., TITTERINGTON, D. M. et al. (2006). Deviance information criteria for missing data models. *Bayesian analysis* **1** 651–673.
- DAUDIN, J.-J., PICARD, F. and ROBIN, S. (2008). A mixture model for random graphs. *Statistics and computing* **18** 173–183.

- DAVIS, A., GARDNER, B. B., GARDNER, M. R. and WARNER, W. L. (1941). *Deep South: A Sociological Anthropological Study of Caste and Class*. University of Chicago Press.
- DOREIAN, P., BATAGELJ, V. and FERLIGOJ, A. (2004). Generalized blockmodeling of two-mode network data. *Social networks* **26** 29–53.
- DURANTE, D. and DUNSON, D. B. (2014). Nonparametric Bayes dynamic modelling of relational data. *Biometrika* **101** 883.
- EVERTON, S. F. (2012). *Disrupting dark networks* **34**. Cambridge University Press.
- FRANK, O. and STRAUSS, D. (1986). Markov graphs. *Journal of the American Statistical Association* **81** 832–842.
- FREEMAN, L. C. (2002). Finding social groups: A meta-analysis of the southern women data. In *In Breiger, R., Carley, C., and Pattison, P. Dynamic Social Network Modeling and Analysis: Workshop Summary and Papers (pp 39–97)*, Washington D.C.: National Research Council, The National Academies Press.
- INTERNATIONAL CRISIS GROUP (2009). Indonesia: Noordin Top’s Support Base. Asia Briefing N 95, (available at: <http://www.refworld.org/docid/4a968a982.html>).
- HANDCOCK, M. S., RAFTERY, A. E. and TANTRUM, J. M. (2007). Model-based clustering for social networks. *Journal of the Royal Statistical Society: Series A (Statistics in Society)* **170** 301–354.
- HOFF, P. D., RAFTERY, A. E. and HANDCOCK, M. S. (2002). Latent space approaches to social network analysis. *Journal of the American Statistical Association* **97** 1090–1098.
- HOLLAND, P. W., LASKEY, K. B. and LEINHARDT, S. (1983). Stochastic blockmodels: First steps. *Social networks* **5** 109–137.
- KOLACZYK, E. D. (2009). *Statistical Analysis of Network Data: Methods and Models*. Springer, New York.
- LEGER, J. (2015). Blockmodels: Latent and Stochastic Block Model Estimation by a ?V-EM?Algorithm. *R package version 1*.
- NEAL, Z. (2014). The backbone of bipartite projections: Inferring relationships from co-authorship, co-sponsorship, co-attendance and other co-behaviors. *Social Networks* **39** 84–97.
- NOWICKI, K. and SNIJDERS, T. A. B. (2001). Estimation and prediction for stochastic blockstructures. *Journal of the American Statistical Association* **96** 1077–1087.
- RAFTERY, A. E., NIU, X., HOFF, P. D. and YEUNG, K. Y. (2012). Fast inference for the latent space network model using a case-control approximate likelihood. *Journal of Computational and Graphical Statistics* **21** 901–919.
- RANCIATI, S., VIROLI, C. and WIT, E. C. (2017). Mixture model with multiple allocations for clustering spatially correlated observations in the analysis of ChIP-Seq data. *Biometrical Journal* doi:10.1002/bimj.201600131. <http://onlinelibrary.wiley.com/doi/10.1002/bimj.201600131/full>.
- RAND, W. M. (1971). Objective criteria for the evaluation of clustering methods. *Journal of the American Statistical association* **66** 846–850.

- ROBINS, G., SNIJDERS, T., WANG, P., HANDCOCK, M. and PATTISON, P. (2007). Recent developments in exponential random graph (p^*) models for social networks. *Social networks* **29** 192–215.
- SEWELL, D. K., CHEN, Y. et al. (2017). Latent Space Approaches to Community Detection in Dynamic Networks. *Bayesian Analysis* **12** 351–377.
- SIGNORELLI, M. and WIT, E. C. (2017). A penalized inference approach to stochastic block modelling of community structure in the Italian Parliament. *Journal of the Royal Statistical Society, Series C (Applied Statistics)* doi:10.1111/rssc.12234. <http://onlinelibrary.wiley.com/doi/10.1111/rssc.12234/full>.
- SPIEGELHALTER, D. J., BEST, N. G., CARLIN, B. P. and VAN DER LINDE, A. (2002). Bayesian measures of model complexity and fit. *Journal of the Royal Statistical Society: Series B (Statistical Methodology)* **64** 583–639.
- WANG, Y. J. and WONG, G. Y. (1987). Stochastic blockmodels for directed graphs. *Journal of the American Statistical Association* **82** 8–19.
- WASSERMAN, S. and FAUST, K. (1994). *Social network analysis: Methods and applications* **8**. Cambridge university press.
- WASSERMAN, S. and PATTISON, P. (1996). Logit models and logistic regressions for social networks: I. An introduction to Markov graphs and p^* . *Psychometrika* **61** 401–425.
- XING, E. P., FU, W., SONG, L. et al. (2010). A state-space mixed membership blockmodel for dynamic network tomography. *The Annals of Applied Statistics* **4** 535–566.

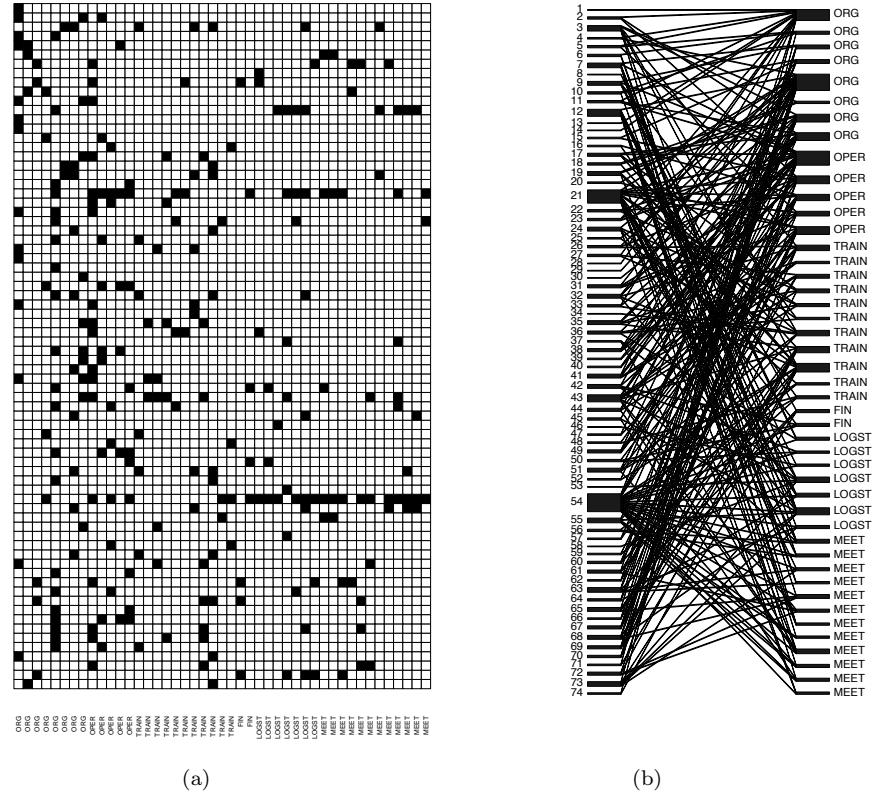


FIG 1. (a) Visualization of the attendances as black boxes for the 74 terrorists (rows) and the 45 events (columns). A black box depicts a connection between a terrorist and an event, while a white box indicates a terrorist not attending that event. (b) Visualization of the attendances as black lines. The width of the left rectangles is proportional to the connections (attendances) of each terrorist to the 45 events, whereas the width of the right rectangles is proportional to the number of terrorist attending each event. Terrorists attending no event are not visualized.

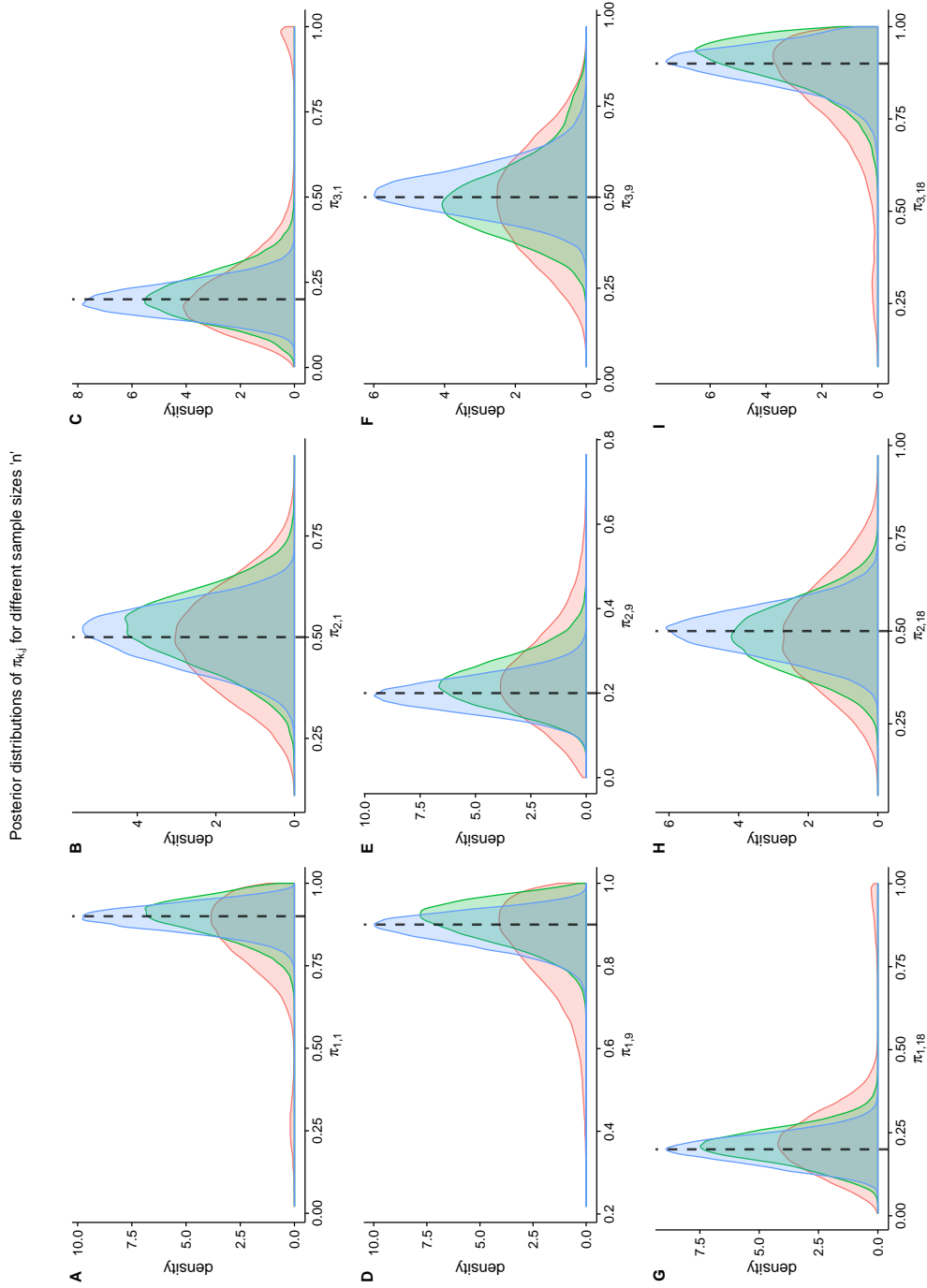


FIG 2. Posterior distributions of $\pi_{k,i}$ for three events $j = \{1, 9, 18\}$ and all the clusters, for varying sample sizes $n = \{100, 250, 500\}$. Each curve collects all posterior samples (after burn-in) from the 25 replicated datasets. The color coding in the plots (A-I) is: red, $n = 100$; green, $n = 250$; blue, $n = 500$. True values of $\pi_{k,i}$ are reported as dashed vertical lines.

Posterior probabilities of allocation

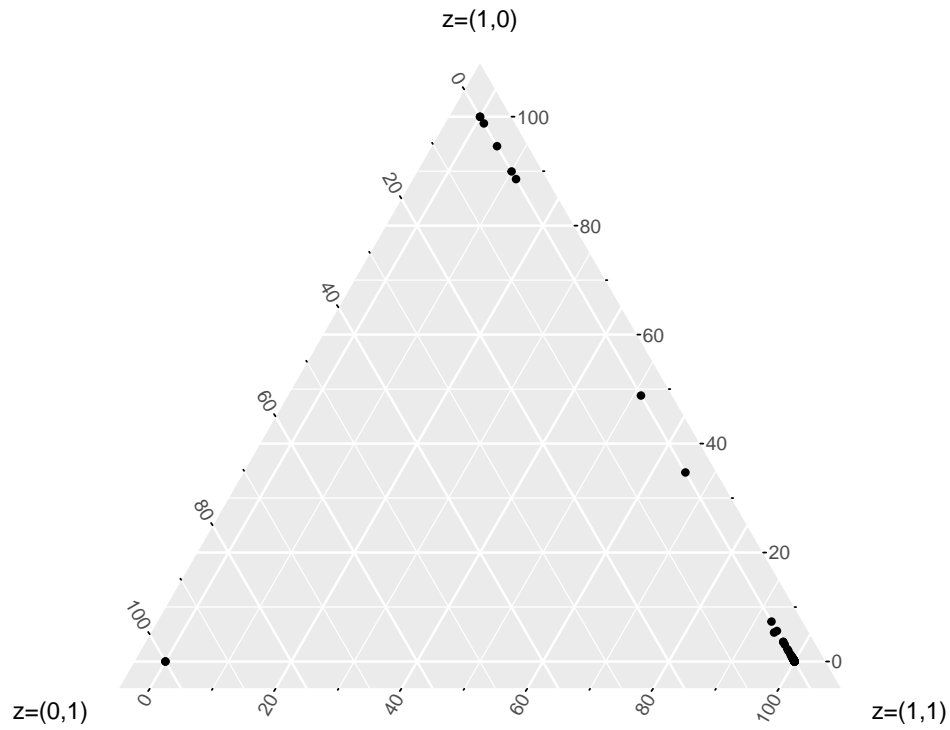


FIG 3. Ternary plot for the (average) posterior probabilities of allocation of each terrorist to each clusters, conditioning on not being in cluster $z = (0,0)$. The 'lone wolves' cluster is omitted for ease of visualization.

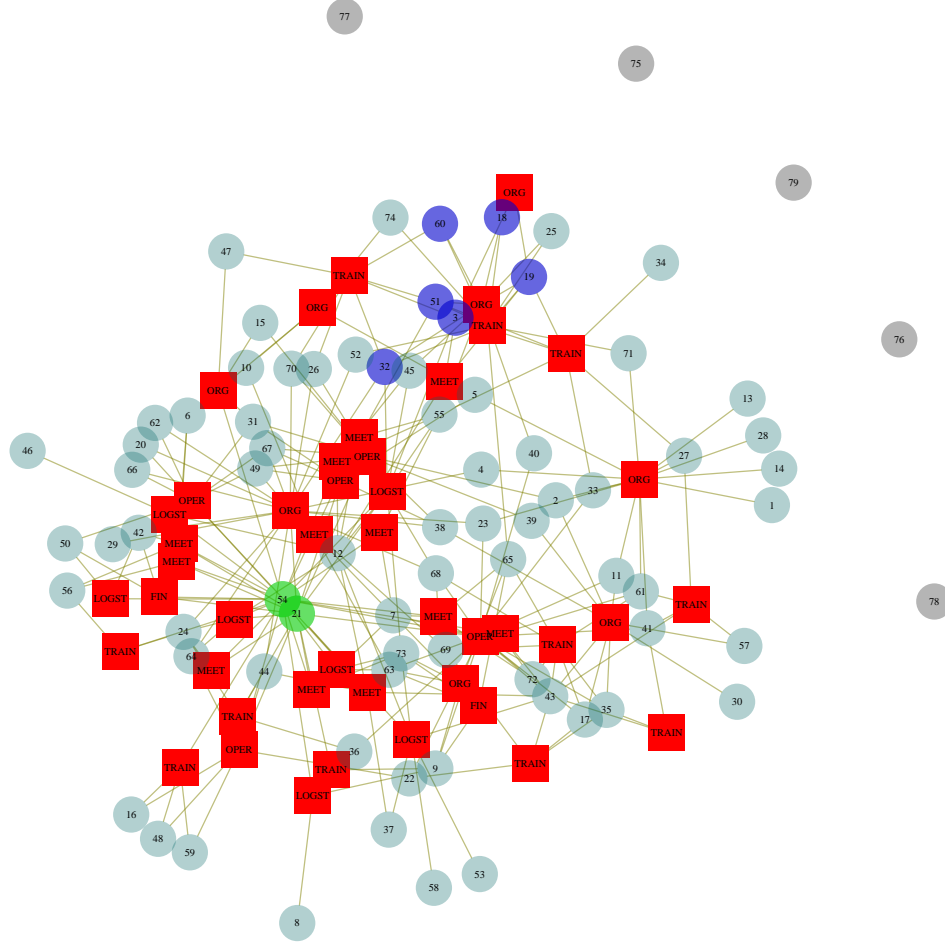


FIG 4. Bipartite (two-mode) representation of Noordin Top terrorists network dataset. Each red square node is an event, with corresponding label, while each circle node is a terrorist (labelled with a progressive number). Color scheme for circle nodes reflects terrorists allocation into clusters obtained by our model *manet*: 2 **green** nodes for cluster $\mathbf{z} = (0, 1)$; 6 **blue** nodes for cluster $\mathbf{z} = (1, 0)$; 66 **light blue** nodes for multiple allocation cluster $\mathbf{z} = (0, 1)$; **grey** nodes $\{75, 76, 77, 78, 79\}$ are the ‘lone wolves’, attending no event.